

FROM PALEO TO POSSIBLE PRESENT-DAY LARGE-SCALE LANDSLIDE. A GENERALIZED NEWMARK APPROACH OF THE TARAPACA LANDSLIDE (NORTHERN CHILE)

José DARROZES¹, Jean-Claude SOULA², Jacques INGLES³ and Rodrigo RIQUELME⁴

ABSTRACT

Paleo-landslides larger than today's are well-preserved in arid areas. Should such large-scale landslides be possible today, much larger devastations than caused by the present-day's greatest registered events could be expected. When the landslide is earthquake-triggered, Newmark analysis allows estimates of the magnitude and site-to-source distance of the seismic event (e.g. Jibson & Keefer, 1993). A generalized Newmark analysis has been developed (Ingles et al., 2006) where ground acceleration is not slope-parallel and the ratio of vertical to horizontal acceleration depends on the seismic situation of the slope. Using this analysis, Arias intensity and the magnitude of earthquakes necessary for large landslides to occur may be markedly lower than expected from the Newmark approach, especially for low-angle slopes with potential deep shear surfaces that are located close to the source of large earthquakes. This approach has been applied to the large-scale Tarapaca paleo-landslide observed in the northern Chile, which is formed on the forelimb of a ~400 km long west-vergent thrust fault-propagation fold (Darrozes et al., 2002). The mechanical and physical characteristics of rocks, slope, climatic changes, seismic activity and the tectonic context being constrained, the analysis indicates that the greatest probability of landslide formation requires either high-magnitude shallow earthquakes situated along the thrust zone not seismically active today (Mw 7.3 at ≤ 15 km to the landslide) or very high magnitude earthquakes situated along active subduction plane (Mw=9.2 at 120 km to the landslide).

Keywords: large-scale landslides; generalized Newmark analysis; Tarapaca (northern Chile)

INTRODUCTION

Landslides are among the most hazardous natural disasters causing heavy loss of human life and economic damages. The largest of the landslides known in the recent past or in the geological record are associated with sector collapse of active volcanoes mobilizing volumes up to several hundred of km³, essentially in form of rock avalanches (Canary Islands: 3500 km³ mostly submarine during the Miocene, Stillmann, 1999; 700 km³ of debris partly offshore at 3 Ma and 100 km³ onshore at 560 ka in Tenerife, Ablay and Hürlihan, 2000; 200 km³ at 560 ka at La Palma and 700 km³ at El Hierro,

¹ Professor, LMTG, OMP, CNRS, University de Toulouse, 14 avenue Edouard Belin, 31400 TOULOUSE, FRANCE, Email: darrozes@lmtg.obs-mip.fr

² Professor, LMTG, OMP, University de Toulouse, 14 avenue Edouard Belin, 31400 TOULOUSE, FRANCE, Email: soula@lmtg.obs-mip.fr

³ Professor, Department of Civil Engineering, University de Toulouse, 118 route de Narbonne, 31400, TOULOUSE, FRANCE.

⁴ Laboratorio de Geoinformática y Teledetección, Departamento de Ciencias Geológicas, Universidad Católica del Norte, Av. Angamos 0610 Antofagasta, CHILE, Email : rriquelme@ucn.cl

Carracedo et al., 1999; Hawaiian range: more than 1000 km³ of debris, Moore et al., 1989, 1994; Garcia et al., 2006). These huge landslides form along relative gentle slopes, affected poorly cohesive materials and were clearly related to volcanic activity.

Table 1. Historical large-scale landslides and geometric parameters associated.

Landslide	Vol. (km ³)	Slope (°)	Travel (head, km)	H _{max} ; L _{max} (km)	Dim. t x L x W _m (km)	Type	Situation	Age	Preservation	Ref.
Fernpass	1.0			1.4; 15.6						Hayashi and Self, 1992
Tamins	1.3			1.3; 13.5						Hayashi and Self, 1992
Siders	1.5			2.4; 17.4						Hayashi and Self, 1992
Engelberg	2.75			1.6; 7.4						Hayashi and Self, 1992
Pamir	2.0			1.5; 6.2						Hayashi and Self, 1992
Saidmarreh	20			1.5; 18.9						Hayashi and Self, 1992
Rondu Mendi Karakoram Himalaya	1.5			>1.7; >10	1.1x4.4x14	Rock avalanche	Valley side	Pre-historic	poor	Hewitt, 1998
Tsergo Ri Central-north Nepal	10	20-25	0.5 - 1	>2.6; 6	0.35(?)x5x10	Rapid rock block slide	River catchment	40 kyr	medium	Ibetsberger, 1996 Schramm et al., 1998
Flims Swiss Alps	12	~25	0.4 – 2.2	2.1; 16.5	0.5x3x5.5	Rapid rock block slide	Valley side	9.8 kyr	Rather good	Pollet, 2004
Köfels Austrian Alps	3.0	20 - 30	0.5 – 0.6	0.5 – 1.4; 6.4	0.5x4.6x3.8	Rapid rock block slide	Valley side	9.8 kyr	Rather good	Pollet, 2004
Thames township New Zealand	1.0	15-25	0.5	0.6; 5.5	0.4x3x1	Soil block slide	Valley side	<< 4.5 Ma (~5 kyr)	Rather good	Moon and Simpson, 2002
Baga Bogd Gobi-Altay, Mongolia	50	3	3 – 4.5	0.4; 21	0.2x20x15	Soil block slide	Mountain front	Pleistocene	Very good	Philip and Ritz, 1999
Lluta Atacama, N. Chile	26	~	~2	~35	0.1-0.3x29x15	Soil block slide	Mountain front	>2.5 Ma	Very good	Stasser and Schlunegger, 2005
Tarapaca Atacama, N Chile	4.0	7.5	0.9	0.6; 5.4	0.2x4.5x7	Soil block slide	Mountain front	≤4.5 Ma	Very good	Darroz et al., 2002 This paper

The largest non-volcanic subaerial giant paleo-landslides are smaller by one or two orders of magnitude than the preceding ones but are markedly larger than the largest historical and recent landslides reported in the literature (see Keefer, 1984, or Voight, 1978) which have volume generally smaller than ~0.5 km³. For convenience, only landslides with volume greater than, or equal to, 1 km³ will be considered here to be mega-landslides (Table 1). These landslides are few in number and located in various parts of either active highly seismic mountain ranges (e.g. Andes, Himalayas) or

ranges having a reduced seismic activity but a high relief due to recent deep fluvial incision (e.g. Alps) (Table 1). Table 1 shows that in active ranges, the mega-landslides may have formed on relatively gentle slopes (15 – 25° or more) but also on slopes as gentle as 3° as in the case of the Baga Bogd landslide which is yet the largest studied (Philip and Ritz, 1999).

The landslides presented in Table 1 have been analyzed from the viewpoint of the geomorphological evolution, the controls of drainage and the production of sediment (Ibetsberger, 1996; Hewitt, 1998; Moon and Simpson, 2002; Philip and Ritz, 1999; Stasser and Schlunegger, 2005; Pollet, 2004), of the mechanisms of displacement and internal structures (Schramm et al., 1998; Pollet, 2004), and of the relationship with active faults (Philip and Ritz, 1999) and pre-existing faults (Schramm et al., 1998; Pollet, 2004; Moon and Simpson, 2002). Philip and Ritz (1999) concluded to the likelihood of a seismic origin of the Baga Bogd landslide on the basis of its size and its association with faults that have been active since at least the late Pleistocene. Limit equilibrium analysis including sensitivity to seismic acceleration, has been performed for the Thames township landslide (Moon and Simpson, 2002). The triggering mechanisms, including seismic shaking, of the other landslides reported in Table 1 have only been considered qualitatively.

As suggested by Jibson (1996), an earthquake origin can be inferred if aseismic failure can reasonably be excluded, even in worst case conditions (maximum piezometric conditions, minimum shear strengths). Dynamic slope-stability analysis can then be used to estimate the minimum shaking conditions that would have been required to cause failure. When the earthquake acceleration time-history is unknown as for the paleo-landslides, back calculations of threshold shaking intensities required to cause catastrophic failure can be used to establish a lower bound magnitude to the triggering earthquake (Jibson and Keefer, 1993). Newmark's permanent displacement analysis constitutes a popular method for determining the magnitude and site-to-source distance of the seismic event necessary for the landslide to form (Jibson and Keefer, 1993). However, one of the limitations of the conventional Newmark analysis is to consider ground acceleration as parallel to the slope, and downslope. To overcome this problem, generalized Newmark analysis (Inglès et al., 2005) has been developed where ground acceleration is not slope-parallel and the ratio of vertical to horizontal acceleration depends on the seismic situation of the slope (magnitude, earthquake source distance, style of faulting).

INGLES ET AL. (2006) GENERALIZED NEWMARK ANALYSIS

Newmark's method (1965)

This method models an earthquake-triggered landslide as a rigid friction block on an inclined plane that is subjected to the same accelerations as the modelled slope. The block will displace when the sum of the static and dynamic forces exceeds the shear resistance of the sliding interface. The slope-parallel critical acceleration required to overcome the shear resistance (a_{cN}) of the block has been defined as a simple function of the static factor of safety and the landslide geometry (Newmark, 1965), expressed as:

$$a_{cN} = (FS-1) \sin \alpha \quad (1)$$

where a_{cN} is the critical acceleration in term of g, the acceleration due to earth's gravity; FS is the static factor of safety; and α the angle from the horizontal that the centre of mass of the potential landslide block first moves.

For the simplest model of an infinite slope (planar slip surface parallel to the slope) the static factor of safety can be expressed as:

$$FS = \frac{c'}{\gamma H \cos \alpha \sin \alpha} + (1 - m \frac{\gamma_w}{\gamma}) \frac{\tan \phi'}{\tan \alpha}, \quad (2)$$

where c' is the effective cohesion, ϕ' is the effective angle of internal friction, γ is the material unit weight, γ_w is the unit weight of water, α is the angle of the slope from the horizontal, H is the vertical depth of the failure surface and m is a ratio of H indicating the height of the ground water table (Fig. 8). The slope is stable for $FS > 1.5$; unstable for $1 > FS \geq 1.5$; and sliding occurs for $FS \leq 1$.

The assumption of infinite slope failure is valid if (1) the landslide mass is thin compared to its length; (2) the failure surface is parallel to the ground surface; (3) failure occurs as basal sliding, which is, in practise, the case of the studied landslides.

In the model of infinite slope, Newmark (1965) considers the ground acceleration a_s to be parallel to the slope and downslope.

Inglès model (2006)

In order to be closer to actual ground shaking conditions, Newmark's approach has been generalised by considering ground acceleration not parallel to the slope (Inglès et al., 2006). In this approach, the ratio of vertical to horizontal components of seismic acceleration $k_1 = a_{sv}/a_{sh}$ depends on the seismic situation of the selected slope (magnitude, earthquake source- distance, style of faulting) and, during the seismic motion, the vertical acceleration acts alternately upslope and downslope.

Uphill motions requiring significantly higher accelerations that are in most cases greater than the peak ground accelerations, only the case of downhill motion has been considered. In this case:

$$a_{Shc} = \frac{(\cos \alpha \tan \phi' - \sin \alpha) + \frac{c'}{\gamma H \cos \alpha} - m \frac{\gamma_w}{\gamma} \cos \alpha \tan \phi'}{k_1 (\cos \alpha \tan \phi' - \sin \alpha) + (\sin \alpha \tan \phi' + \cos \alpha)}, \quad (3)$$

where a_{Shc} is the horizontal critical acceleration needed to reduce the pseudo-static factor of safety to 1.0, expressed in term of g . Newmark's model corresponds to the particular case where $k_1 = -\tan \alpha$ of this general model.

Attenuation relationships

Several empirical attenuations relationships for predicting free-field vertical component of peak ground acceleration (PGA) in terms of magnitude, source-distance, sites conditions and style of faulting have been developed (Abrahamson and Litehiser, 1989; Campbell, 1989; Campbell, 1997; Ambraseys and Simpson, 1996). These attenuation relationships have been used to predict near-source vertical ground motions for engineering purposes.

Seismic building codes, such as Uniform Building Code or Eurocode 8, generally assume that the peak vertical acceleration is simply a fraction of the peak horizontal acceleration. A value of two-thirds is most often used as the maximum effective ratio between vertical and horizontal acceleration (Newmark and Hall, 1982). In 'Eurocode 8 'Design Provisions for Earthquake Resistance of Structures', this ratio is fixed to 0.9 in regions where the magnitude $M > 5.5$ and to 0.45 where $M < 5.5$. Analyses of earthquake-triggered landslides need calculations of the cumulative displacement.

The empirical relationship established by Jibson (1993) based on Arias intensity (I_a) takes the following form:

$$\log D_N = 1.460 \log I_a - 6.642 a_{cN} + 1.546, \quad (4a)$$

where D_N (Newmark's displacement) is in centimetres, I_a in metres per second and a_{cN} (Newmark's critical acceleration) in fraction of g .

This relation has been slightly modified by Jibson et al. (1998):

$$\log D_N = 1.521 \log I_a - 1.993 \log a_{cN} - 1.546, \quad (4b)$$

From Californian earthquakes, Wilson and Keefer (1985) suggested the following simple empirical relationship to predict Arias intensity as a function of earthquake magnitude and source distance:

$$\log I_a = M - 2 \log R - 4.1 + 0.44P, \quad (5)$$

where I_a is in metres per second, M is moment magnitude, R is earthquake source- distance in kilometres, and P is the probability, in probits, of the actual I_a exceeding the predicted I_a . In the same manner as k_1 , Arias intensity depends on the seismic situation of the potential landslide (Magnitude M ; distance to the source R).

Because the seismic horizontal acceleration a_{Sch} in Inglès et al.'s (2005) model is in most cases smaller than Newmark's critical acceleration a_{cN} , the cumulative displacement D inferred from this model will be greater than D_N and the conditions of instability attained for lower magnitude events. The difference may be considerable, particularly for low-angle slopes with potential deep shear surfaces that are located close to the source of great earthquakes.

Using relations (1), (3), and (4a) we can calculate the ratio $K_D = D/D_N$. It can be shown that K_D is independent of I_a and takes the following form:

$$\log K_D = 6.642 a_{Sch} (K_{ac} - 1), \quad (6)$$

where $K_{ac} = a_{cN}/a_{Sch}$. Inglès et al. (2005) found it more convenient to make use of Jibson's (1993) formulation (Eq. (4a)) considering that Jibson's et al. (1998) formulation does not provide significant improvements for the purpose of their analysis.

If the critical acceleration can be determined and a critical displacement estimated, then relation (4a) can be used to estimate the threshold Arias intensity required to initiate failure. Critical displacement is defined as the coseismic displacement beyond which a general failure of the landslide mass may occur. Masses that display brittle behaviour have a lower critical displacement, generally assumed as 5 cm (Wieczorek et al., 1985), than masses whose ductility accommodates greater deformation prior to sliding, generally assumed to be 10 cm (Jibson and Keefer, 1993). Relation (5) leads then to a relation between magnitude and earthquake source distance. When the seismic source zone is well documented, this distance can be determined and relation (5) will yield a reasonable minimum magnitude estimate for the triggering earthquake.

THE TARAPACA LANDSLIDE

The mega-landslides of the "Moquella flexure".

Not surprisingly, Table 1 shows that the state of preservation of the landslides is closely related to climate. This explains why even recent landslides are poorly preserved in wet climates (Alps, eastern Himalaya) and why smaller-scale landslides of the same age are rarely recognized in this context. The well-preserved landslides of arid areas are therefore better suited for analyzing the triggering mechanisms. In the present paper, we have chosen to analyse the Tarapaca landslide which is one of a series of large-scale landslides formed in the Atacama Desert along the western flank of N-S trending thrust-related "flexures" in the Precordillera of northern Chile and southern Peru. These landslides are well preserved because of the limited fluctuations of the climate which has been arid all along the late Cenozoic (Alpers et al., 1988; Gregory-Wodzichi, 2000) with one of the lowest rainfall in the world, estimated at 4 mm/y during the last century (Vargas et al., 2000), and of the limited anthropic activity.

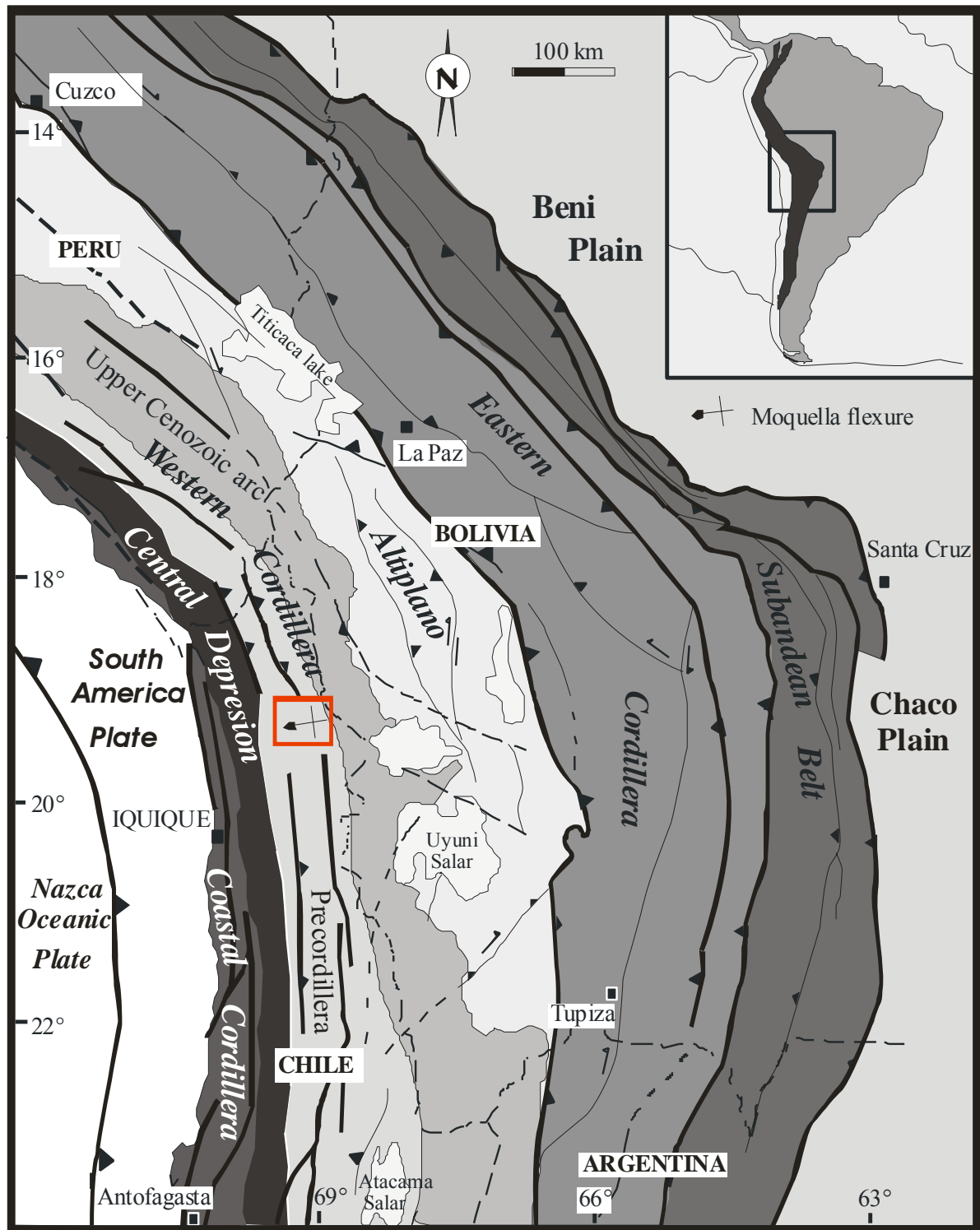


Figure 1. Tectonic sketch map modified after Hérail (1996), red box identified the studied landslide

The Tarapaca area (Fig. 1 & 2) is situated near Iquique (19°55S, 69°35W) in late Cenozoic syntectonic deposits on the forelimb of the 'Moquella fault-propagation fold' (Fig. 3). The syntectonic strata unconformably overlay a basement made up of deformed Mesozoic sedimentary and intrusive rocks (Fig. 3 & 4). These syntectonic strata (Fig. 4) include 4 units. Unit A comprises consolidated fluvial deposits with five intercalations of ignimbrites. Units B, C and D are poorly cemented. Unit B shows ignimbrite intercalations whose thickness decreases westward. Two main 'ignimbrite' layers,

the Nama and the Tarapaca, have been identified. The Nama 'ignimbrite' is in fact a welded tuff ~200m thick. It consists of 15-20 vol.% Plagioclase, 2 vol.% Quartz, 5 vol. % Biotite, 2 vol. % Pyroxene and Amphibole 1 vol.% opaque minerals, and 75-70 vol.% volcanic glass. K-Ar dating of biotite gives 16.02 ± 0.7 Ma (Muñoz et al., 1992).

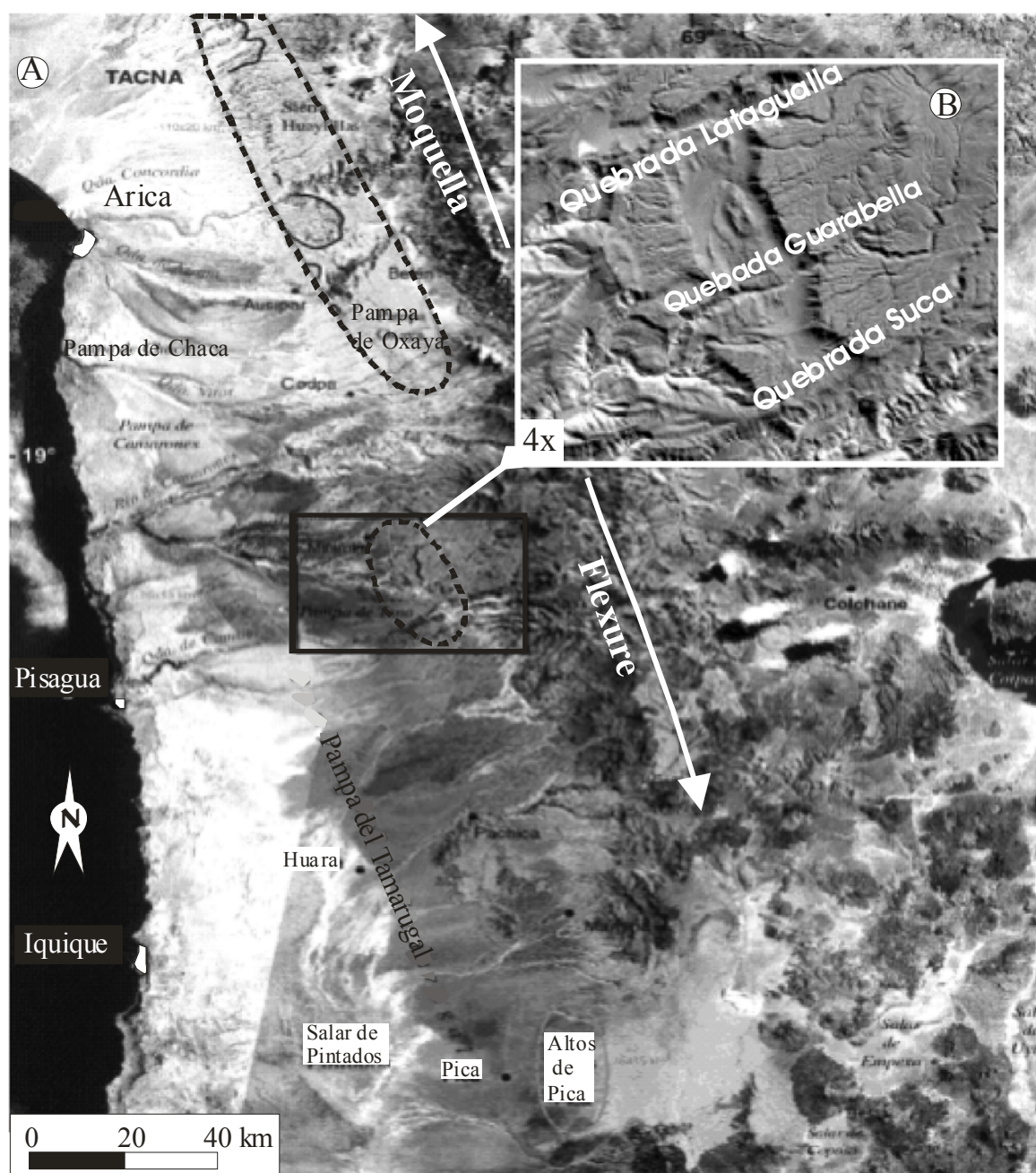


Figure 2. Multispectral imageries of the studied area A) Regional Landsat TM image (res. = 28.5m) and highlighted landslides (dot lines), B) ASTER image of the Tarapaca landslide. (res. = 15 m)

The Tarapaca ignimbrite is an ignimbritic tuff ≤ 40 m thick (Fig. 4A). Its composition is similar to that of Nama and K-Ar dating on biotite yields 16.3 ± 0.6 Ma (Muñoz et al., 1992). The sedimentary deposits are predominantly stratified arenites alternating with thin argillaceous sands. Unit C is constituted by coarsening-upward gravel-bearing sands. Unit D is made up of grain-supported gravels. Unit E is an andesitic lava flow unconformably resting over Units D to A (Fig. 4).

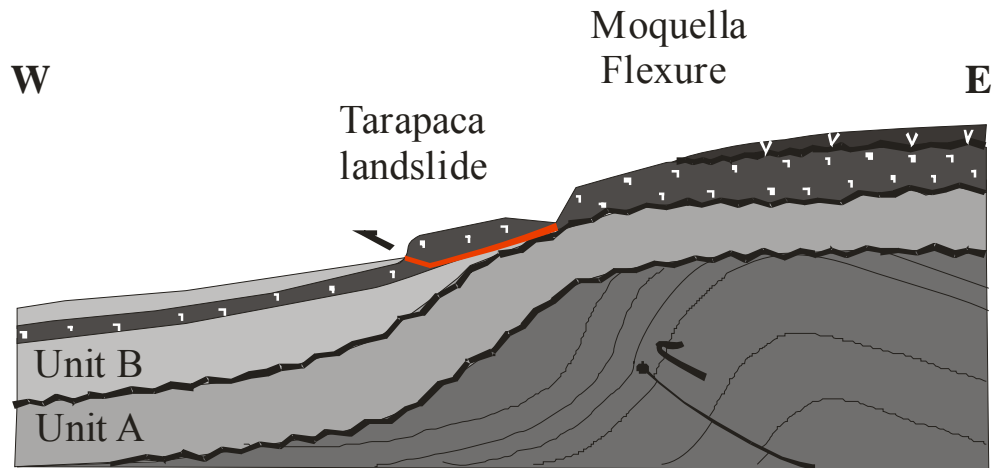


Figure 3. Schematic profile of Moquella flexure, the failure is located at the base level of ignimbritic material (dark gray with blank dot), the unit A and B are syntectonic material associated to the Moquella blind thrust activity. A more detailed stratigraphic sequence is defined in figure 4.

All the mega-landslides located on the western limb of the Moquella flexure have a planar basal sliding surface where initiating at the interface between two layers. More rarely, the slip surface is curved but the curvature remains small. All these landslides display a slip length much greater than the thickness. For example, the thickness D of the Tarapaca landslide is 200 m and its slip length L is 2375 m. This arrives to a ratio D/L of 0.094 much lower than the value of 0.15 that separates rotational from translational slide according to Skempton and Hutchinson's criterion (Skempton and Hutchinson, 1969). The slope of the landslides varies between 8 and 5° and their area between 20 and 40 km².

Morphology of the Tarapaca landslide

The structure of the Tarapaca landslide is well exposed in the Suca, Lataguella, and Guarabella Rivers sections (Fig. 5). Its basal shear plane is localized in a clay layer at the base of the Tarapaca ignimbrite (Fig. 4) and has one of the most important slopes of the landslides from the Atacama Desert (7-8°). The volume of the slumped mass has been estimated to be 4.503 ± 0.03 km³. The transported mass was the Tarapaca and Nama ignimbrite-dominated formations that constitute the load of the landslide. The main scarp of the landslide can easily be identified on the map (Fig. 5). It has a length of ≈ 7 km and an elevation close to 200 m. This elevation corresponds approximately to the total thickness of the transported ignimbrites. The landslide is limited by the Quebradas Suca to the north and the Quebrada Lataguella to the south and is separated into 3 blocks. The Quebrada Guarabella separates block #1 from blocks #2 and #3 (Figs. 5, 6, 7). Differential displacement along the Quebrada Guarabella varies from ~ 600 m at the head to ~ 800 m at the toe. Rare edge-parallel strike-slip faults, showing little differential displacement, are observed in the main body. The most prominent of these separates blocks #2 and #3, with a differential displacement smaller than 100 m. Edge-parallel strike-slip shear zones form in block #1, allowing a larger displacement of the central part of this block. Some minor scarps along tilted NE-SW normal faults parallel to the main escarpment can be observed in the head of the landslide, especially in block #1. In the centre of block #1 where landslide displacement was larger, a small internal antiformal thrust stack with opposite vergences formed in the foot as a result of damping of the slide mass. In front of this pop-up is observed a small lagoon filled with marly evaporites. This lagoon probably formed at first in the backlimb of the frontal accumulation ridge and was then disconnected from upstream water sources by the ejection of the pop-up and dried. A small secondary landslide also formed in the foot zone because of the instability of the overlapping mass resulting from the increase in slope (Fig. 5A).

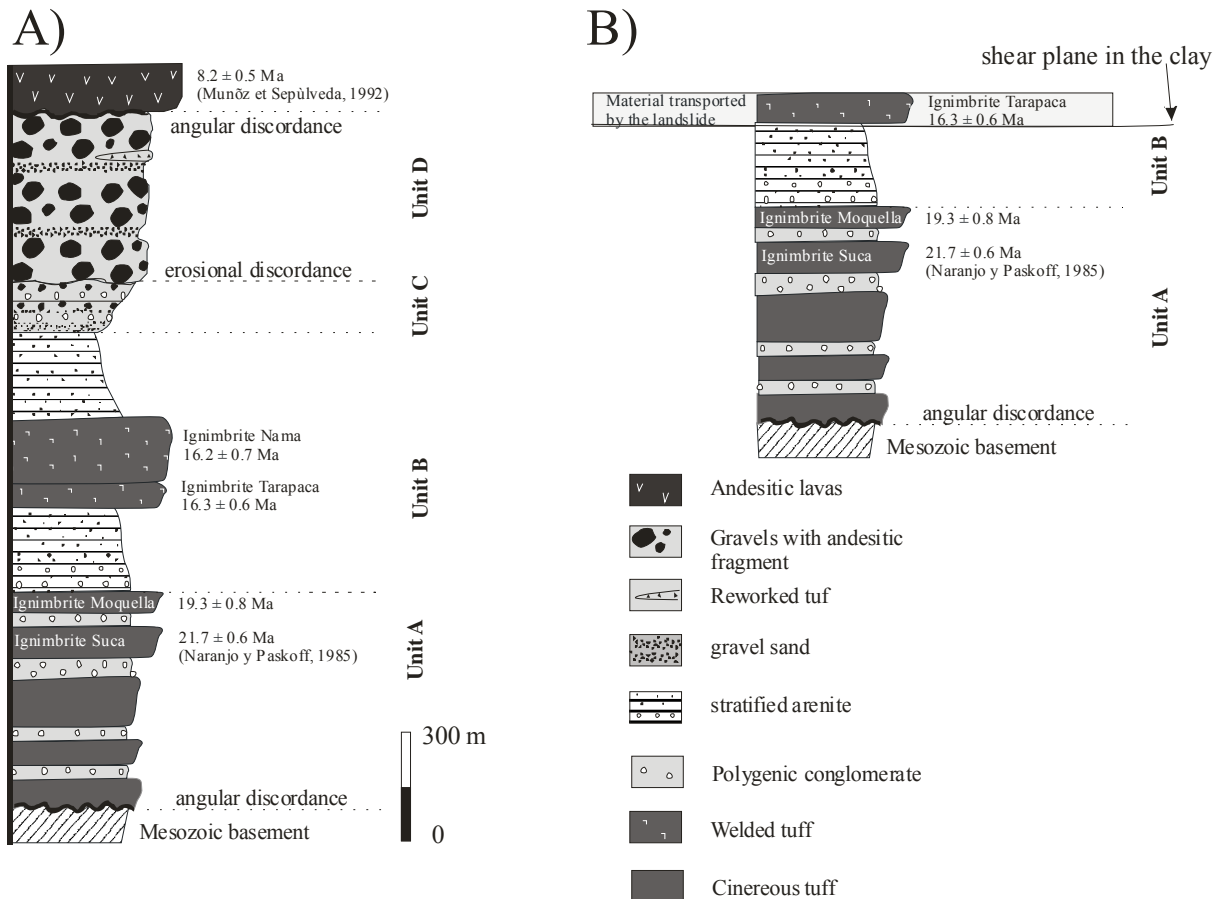


Figure 4. Synthetic stratigraphic column of the different units A) for the studied area; B) for the Tarapaca landslide.

Relationship between the Tarapaca landslide and the drainage network

The drainage network in the Tarapaca area is dominated by rivers flowing toward the west-south-west (Figs. 2, 5A). The deeply incised east-west flowing Suca and Lataguella rivers constitute the northern and southern boundaries of the landslide. Except the Guarabella River that separates two independent blocks in the landslide and allowed differential displacements of these blocks (Figs. 5A & 6A), there are no along-slope rivers and no tributaries traversing the landslide. Whereas the tributaries to the main rivers form an undisturbed drainage pattern on both sides out of the landslide, those tributaries that flowed toward the landslide are interrupted by the main escarpment. Upstream of the main escarpment, some of these rivers were diverted along landslide-related normal faults. This demonstrates that the installation of the drainage network predated landsliding. According to Naranjo and Paskoff (1985), this drainage network was initiated 5.5 My ago, which means that landsliding was younger than 5.5 Ma. The main rivers such as the Suca, Lataguella, and Guarabella Rivers can be interpreted as antecedent rivers favouring landsliding by preserving free edges to the future gliding layer. Streamlets incising the landslide foot develop no headward erosion that outpaces the elevated shortened zone. This indicates that the installation of a very immature drainage network within the landslide structure occurred only recently.

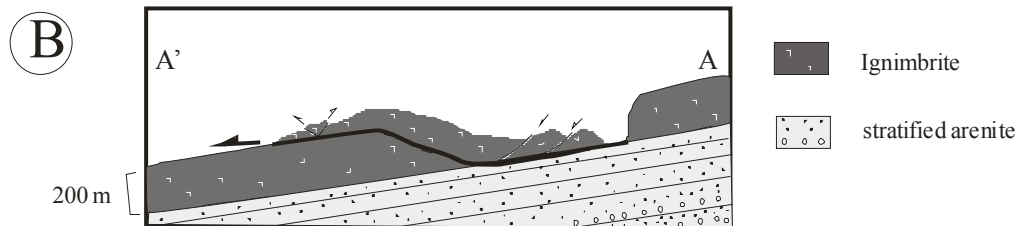
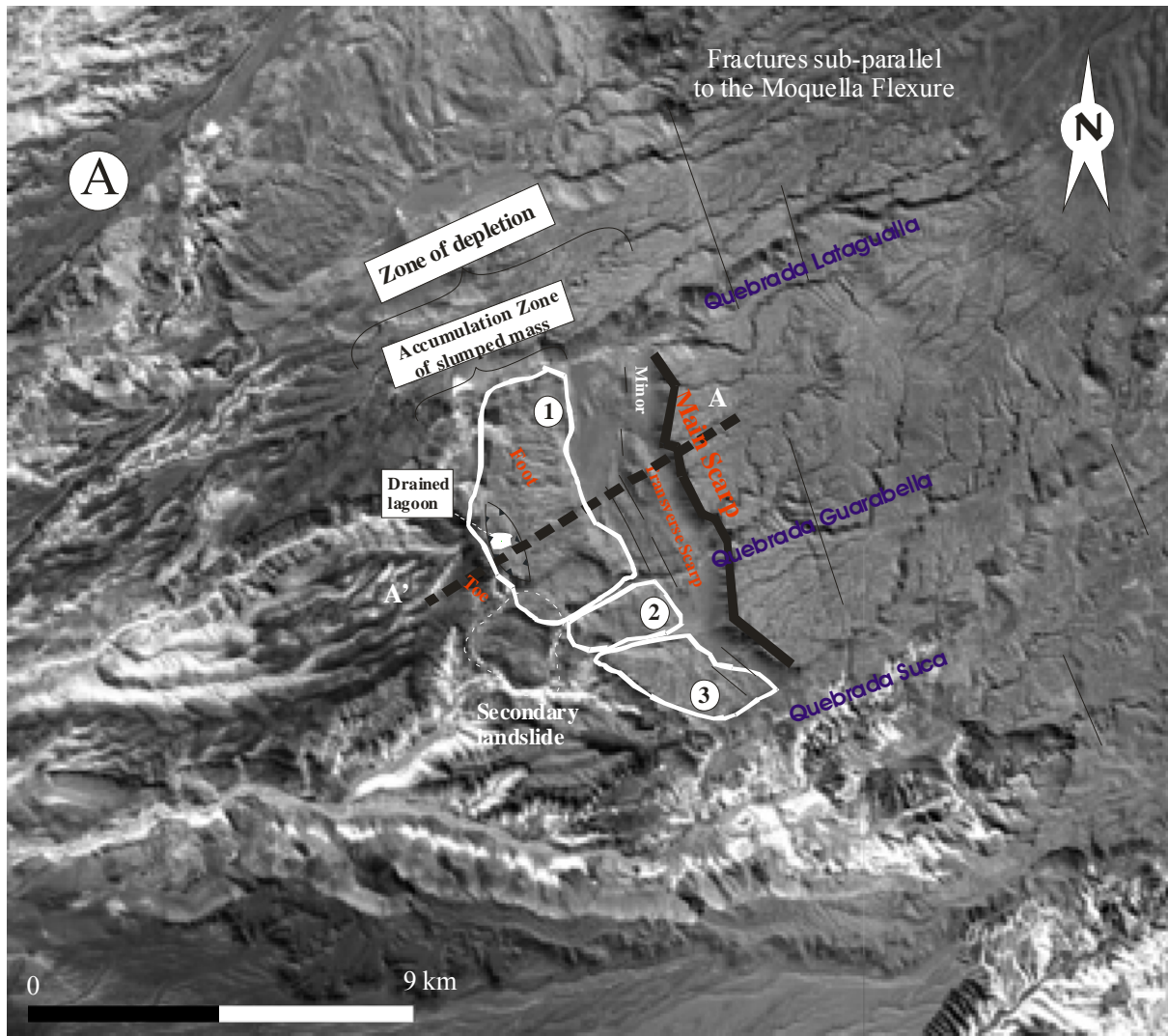


Figure 5. Major morphological and structural features of the Tarapaca landslide : A) Aster VNIR image (resolution: 15m); dotted line = location of the B) schematic profile of the landslide

Analysis of the parameters influencing the rupture of the Tarapaca landslide

Table 2 presents an overview of the factors facilitating or preventing landslides. In our case, the determining parameters are (1) the increase in slope due to tectonics, (2) water pressure even though the amount of water available is small and seepage occurs very temporarily during storms, (3) removal of lateral support, and (4) earthquakes. In the following, we will examine first the effect of the static (aseismic) mechanical/physical characteristics of the landslide material coupled with the climatic factors expressed by changes in pore-water pressure. The effect of earthquake shaking will be then considered.

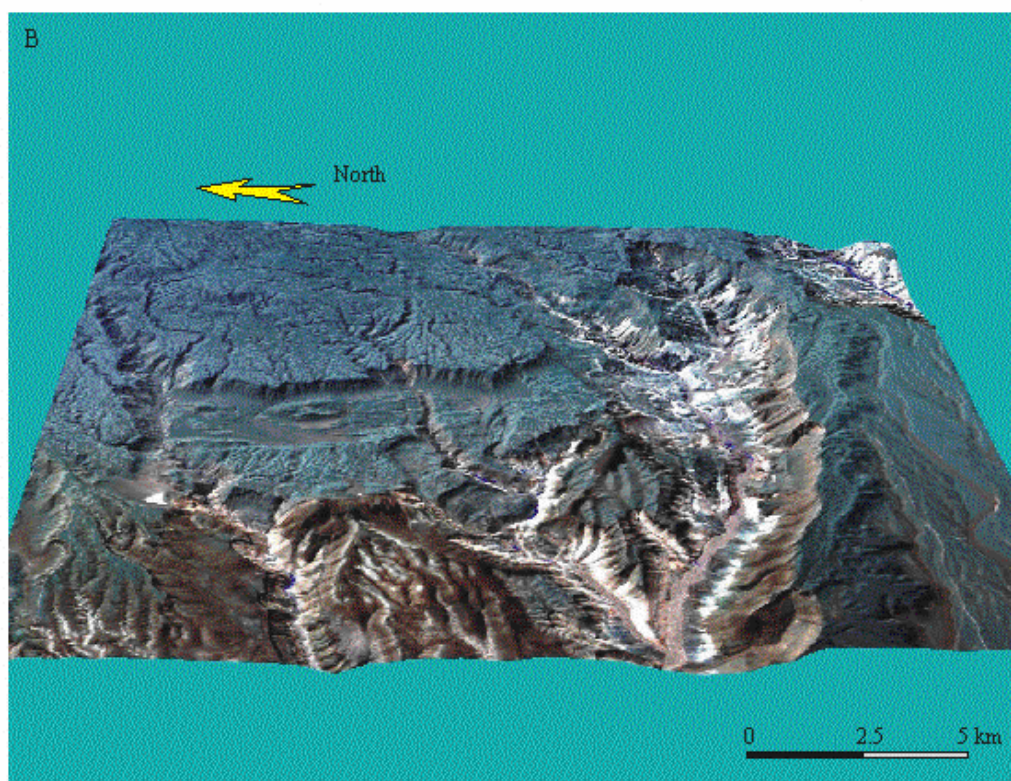
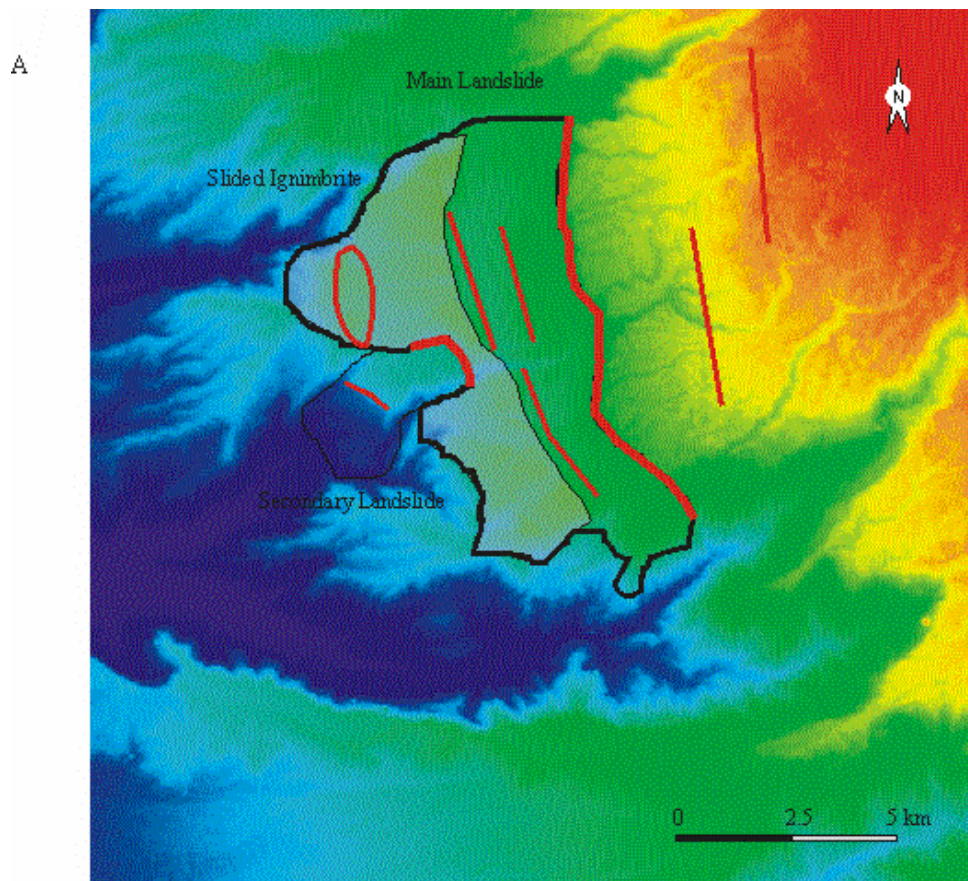


Figure 6. DEM of the Moquella flexure: a) DEM build using stereographic pair of Aster images (map res. = 15m, altitudes vary between 900m asl, in the western part to 4400m for the eastern zone. For the landslide, the altitude ranges are around 1500m, at the SW, to 2800m, at the NE; b) The 3D View is building using the Aster DEM and the multispectral ASTER images.

Table 2. Factors facilitating or preventing landslides, modified after Summerfield, 1991

Factor	Examples
<i>Factors contributing to increase the shear stress</i>	
Removal of lateral support through undercutting or slope stepping	Erosion by river and glaciers, wave action, faulting, previous rock fall or slide
Removal of underlying support	Undercutting by river, loss of strength by extrusion of underlying sediments.
Loading of slope	Weight of water, accumulation of debris
Transient stress	Earthquakes
<i>Factors contributing to reduce the shear strength</i>	
Weathering effect	Dissolution of cementing mineral in rock, disintegration of granular rock
Changes in pore-water pressure	Saturation, softening of material
Changes of structure	Creation of fissures
Organic effects	Burrowing of animals

Mechanical static parameters and climatic factors

For the simplest model of an infinite slope (planar slip surface parallel to the slope) applicable to the Tarapaca landslide, the aseismic (static) factor of safety can be expressed by the relation (2). The climatic factor is represented by the pore pressure in the sediment. This is expressed in equation (2) by the ratio m , which may vary from 0 (dry conditions) to 1 (saturated conditions).

In the studied case, we have determined the slope angle $\alpha = 7^\circ \pm 1.5^\circ$ and the vertical depth $H = 200 \text{ m} \pm 10 \text{ m}$. The values of the other parameters can be estimated using published data from the Table 3 for common rocks. In order to analyze the possible causes of landsliding, different scenarios have been established, using different values for c' , ϕ' , γ and m (Figs. 8 & 9). Effective cohesion c' has been assumed to vary from 30 to 100 kPa for clayey rock. This corresponds to the cohesion of a soap layer capable of allowing landsliding. The unit weight of the Tarapaca ignimbrite varies as a function of weathering from 15 kNm^{-3} for a powdery tuff to 23 kNm^{-3} for a poorly consolidated tuff. The angle of effective internal friction has been taken to vary from 25° (gypsum-bearing clays) to 50° (crushed gravel mixture). Unit weight of water, γ_w , is taken as 10 kNm^{-3} .

Table 3. Range for strength parameters of common rocks, modified after Hoek and Bray, 1981.

Material Groups	$c'(\text{kPa})$	$\phi(^{\circ})$	$\gamma(\text{kN/m}^3)$
Dry sands, Colluviums, Soft sandstone, conglomerate and clayey rock	0-100	25-34	15-20
Weathered Tuff, Tuff, Volcanic rock	30-300	30-65	19-27
Firm sandstone and clayey rock	100-150	45-50	21-24
Siliceous rock	25-100	45-64	26
Well-bedded, Hard to Firm sandstone and clayey rock	75-100	27-38	21
Mixed clayey sheared rock, hard block, and masses of hard rock	35-50	20-30	21
Deformed hard sandstone and clayey rock	50-100	27-38	21
Hard homogenous rock	100-300	50-64	27

The first scenario (A) of Figure 9 illustrates the loading effect through the variation of unit weight γ , assuming a constant thickness and a constant slope angle. This shows that changes in γ do not modify significantly slope stability except for unrealistic condition ($\gamma < 3 \text{ kN/m}^3$). The static factor of safety resulting from realistic conditions ($c' = 30\text{--}100 \text{ kPa}$, $\phi' = 35^\circ$, $\gamma = 15\text{--}23 \text{ kNm}^{-3}$) ranges between 6 to 4 for slope angle varying between 5.5 to 8.5° , which indicate the perfect stability of the load for a slope angle of $7^\circ \pm 1.5^\circ$ as measured in the field.

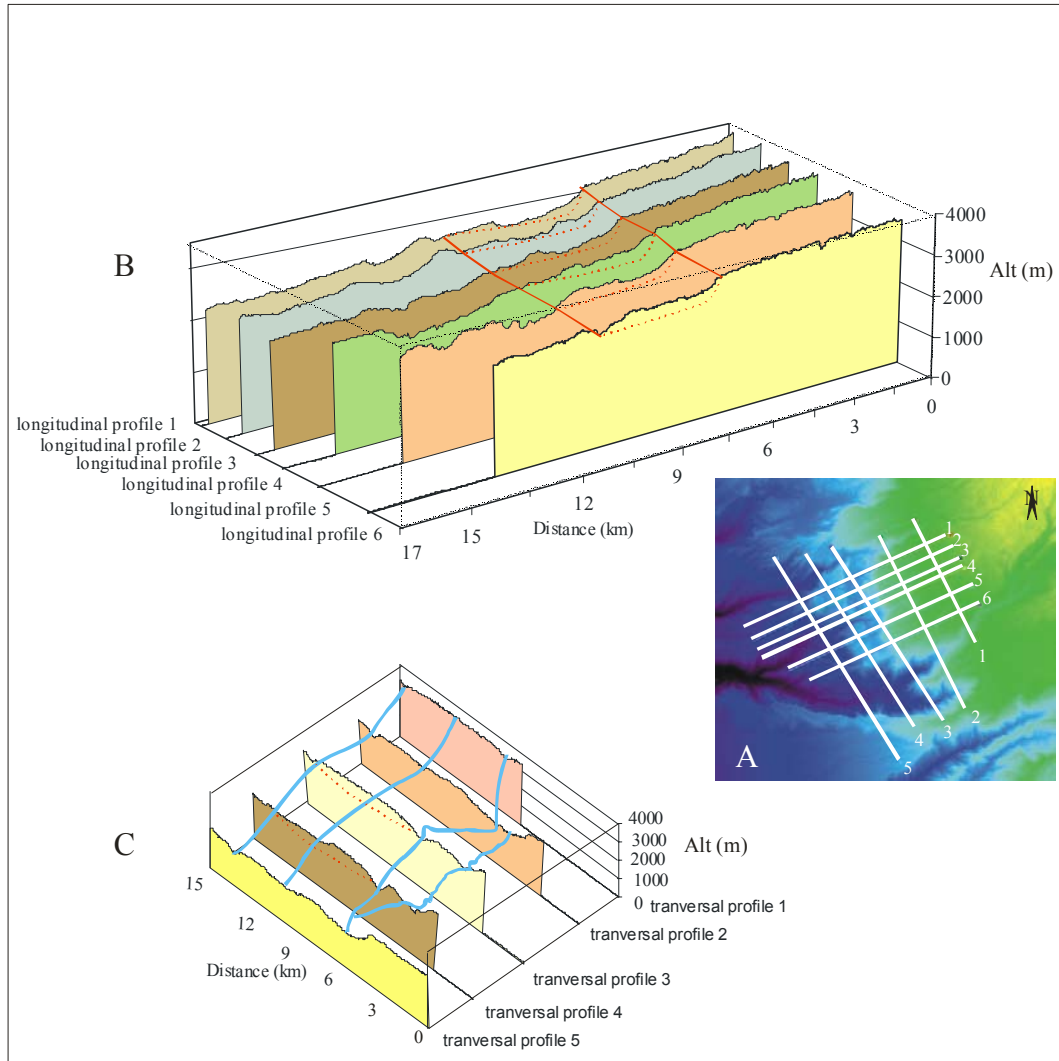


Figure 7. Topographic profiles of the Tarapaca landslide (red lines), A) location map of B) longitudinal profiles, C) transversal profiles. The origin of longitudinal profile is defined by the profile #1 $x=0$ at the eastern part and for transversal ones by the profile #5 $x=0$ at the southern part.

The second scenario (Fig. 9B) analyses the effect of changes in cohesion on the safety factor and slope stability, using $m = 0$ (no water present). The other conditions are $\alpha = 7^\circ$, $H = 200$ m as established from the field study. This shows that the safety factor and slope stability are relatively insensitive to cohesion.

The third scenario (Fig. 9C) analyses the effect of changes in internal friction angle ϕ . For small internal friction angles ($\phi < 10^\circ$) the slope is unstable; for large angles ($\phi > 60^\circ$), the load becomes irremovable. For angles of $35-50^\circ$ as in the studied example, the load is stable (FS has an average value of 4).

The last scenario (Fig. 9D) illustrates the influence of changes in ground water pressure. The safety factor reduces by a factor ≈ 2 when changing from $m = 0$ (dry conditions) to $m = 1.0$ (wet conditions). The latter value of $m = 1.0$ is assumed to represent the effect of water seepage due to short-duration severe storms in a previously water-free high-porosity rock. Since the climatic factor influencing slope stability is essentially marked by ground water pressure changes in sediments, this indicates that, in

the studied example, even severe storms are not sufficient by themselves to destabilize the load.

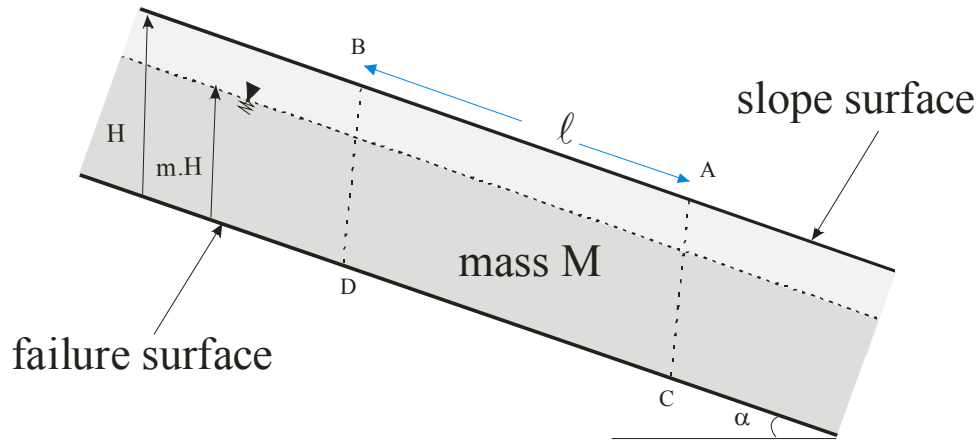


Figure 8. The model of infinite slope; the mass of the sliding block ABCD is M.

Earthquakes

The aseismic safety factor predicting slope stability even for the most severe possible conditions, earthquake shaking is now to be considered.

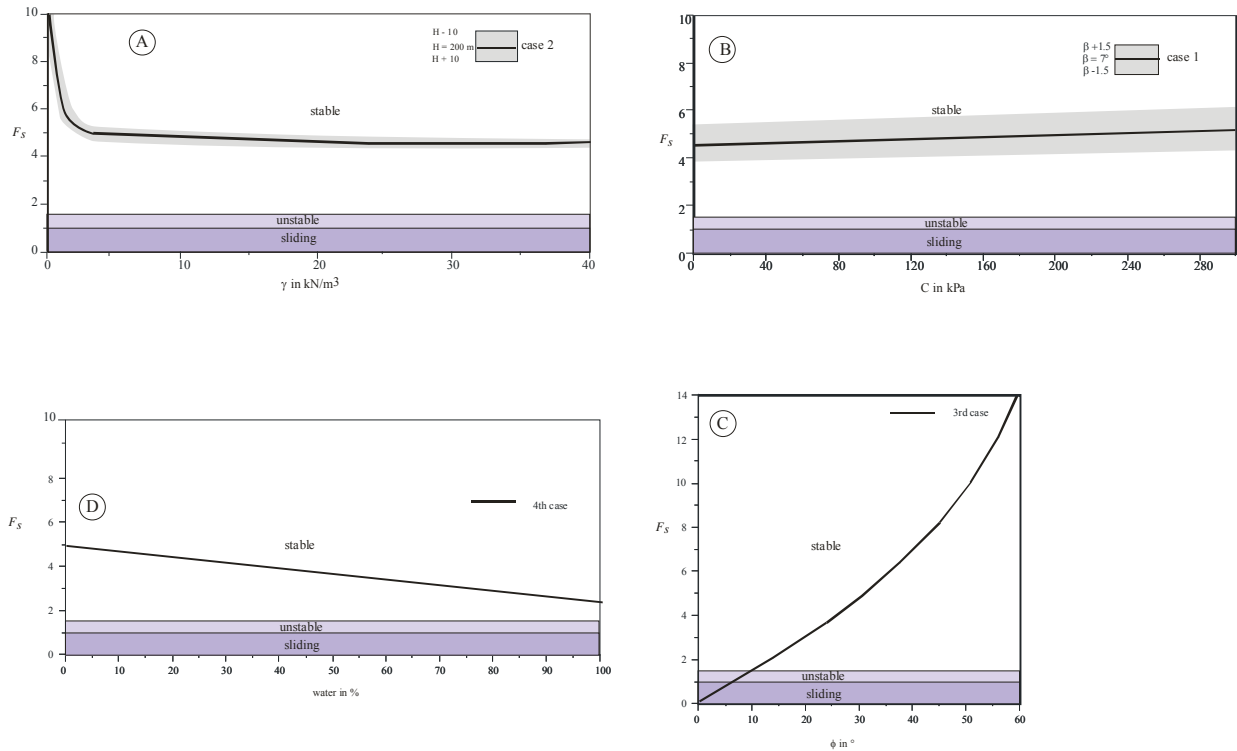


Figure 9. Parameters influencing the slope stability; A) alteration, B) load, C) internal friction angle and D) ground water table. Dashed lines correspond to theoretical value not available in our case.

The characteristics of the Tarapaca landslide: large volume, low-angle and deep-seated basal shear surface, materials having a relatively high strength strongly suggest that the landslide was triggered by strong and probably long duration earthquake shaking (high magnitude and large Arias intensity). However, because of the depth of the failure surface, the term of cohesion (c'/H) is rather small. This and the low-angle and deep-seated basal shear surface correspond to a large ration (K_{ac}) of Newmark's

critical acceleration (a_{cN}) to seismic horizontal acceleration as defined by Inglès et al. (2005). Back calculations of threshold shaking intensities will result in lower Arias intensity and lower magnitudes. Arias intensities and moment magnitudes have been calculated for the Tarapaca landslides using Inglès et al.'s (2005) model, the characteristics of the materials being those defined in the calculations of the aseismic safety factor ($\alpha = 7^\circ$; $H = 200$ m; $m = 0.5$; $c' = 30 - 100$ kPa; $\gamma = 15 - 23$ kPa; $\phi' = 35^\circ$). The critical displacement was assumed to be 10 cm. These calculations indicate Arias intensity of 16.84 m/s and moment magnitudes of $M_w = 6.98$ at 15 km to the landslide, $M_w = 8.26$ at 50 km to the landslide and $M_w = 9.2$ at 120 km to the landslide. As a comparison, the conventional Newmark analysis would have given moment magnitudes of $M_w = 7.65$; $M_w = 9.23$ (exceptional) and $M_w = 10.38$ (unrealistic) and unrealistically high Arias intensities of 32.49 m/s.

DISCUSSION

Influence of climate

The mega-landslides described in Table 1 are rare events, the youngest ones being aged of 9500 yr (early Holocene). This indicates that the recurrence time is at least ~ 10 kyr. These mega-landslides formed along relatively gentle ($15 - 25^\circ$ or more) slopes but along mild to almost horizontal (8 to 3°) slopes as well. Table 1 also shows that the more recent registered mega-landslides are poorly preserved and that the best preserved are low-angle soil block slides with ages between 5.5 and 2.5 Myr in the Atacama Desert (Strasser and Schlunegger; this paper) and late Pleistocene in the Gobi Desert (Philip and Ritz, 1999). This apparent paradox is easily explained when considering that erosion has remained weak in these arid areas whereas it was much intense in the wet climates of the Himalayas and the Alps. Moreover, erosion is obviously less efficient in the gentle slopes of mountain piedmonts than in the relatively gentle slopes of deeply incised valleys of the hinterland. The best-suited landslides for slope stability analyses are therefore those preserved in arid areas.

If the above calculations show that the formation of gently sloping large-scale landslides such as the Tarapaca landslide analysed here needs earthquake shaking for any value of pore-water pressure, the influence of climate may, however, be non-negligible. Equation (3) shows that pore-water pressure will reduce the safety factor in the case of earthquake shaking as in the case of a static load (equation (2)), which indicates that for higher pore-water pressure, lower magnitude earthquakes are needed to trigger landsliding. In very arid areas such as Atacama Desert, however, increase in pore-water pressure is limited by the relatively low rate of water seepage and the short duration of the storms, which cause most of the rain water to be dissipated by runoff and evaporation.

Distant climate reigning in the high-elevation regions east of the studied area seems more efficient for landslide initiation than the severe but rare storms occurring in the arid area. As stressed by Strasser and Schlunegger for the nearby Lluta landslide, an overpressure resulting from seepage originating from the more humid Western Cordillera is highly unlikely because of the deeply penetrating longitudinal thrust faults upstream of the landslides. However, the absence of lateral support to the landslide resulting from deep incision by transverse rivers is the most important contribution of climate to enhance landsliding and is implicit in the calculation of the safety factor using the infinite slope model. Although fundamentally caused by tectonic uplift and lowering of the local base level, deep incision of river valleys removing lateral support to the sliding mass is possible in this arid climate only because of the high water discharge of the main rivers whose catchment is situated near the volcanoes of the Western Cordillera. These volcanoes exceed 4500m asl and the relieves that form a barrier for moisture coming from the Amazonian basin store this moisture in the form of snow or rain (Aceituno, 1993). Moreover, the observation that the studied large-scale landslides are systematically bounded by rivers issued from the high-elevation humid areas should indicate that gently-sloping large-scale landslides may not have formed if these rivers were absent.

Magnitude and location of the possible landslide-triggering earthquakes

All the scenarios taking into account realistic variations of the static (aseismic) mechanical

characteristics of the landslide-involved material and pore pressure values compatible with the climate of the area, including effects of severe storms, indicate slope stability. Therefore, earthquake shaking is necessary to the formation of these gently-sloping large-scale landslides. The high degree of preservation of the Tarapaca landslide and other similar landslides formed along the Moquella thrust enables them to be used as a proxy for determining the magnitude and the possible locations of the paleo-earthquakes.

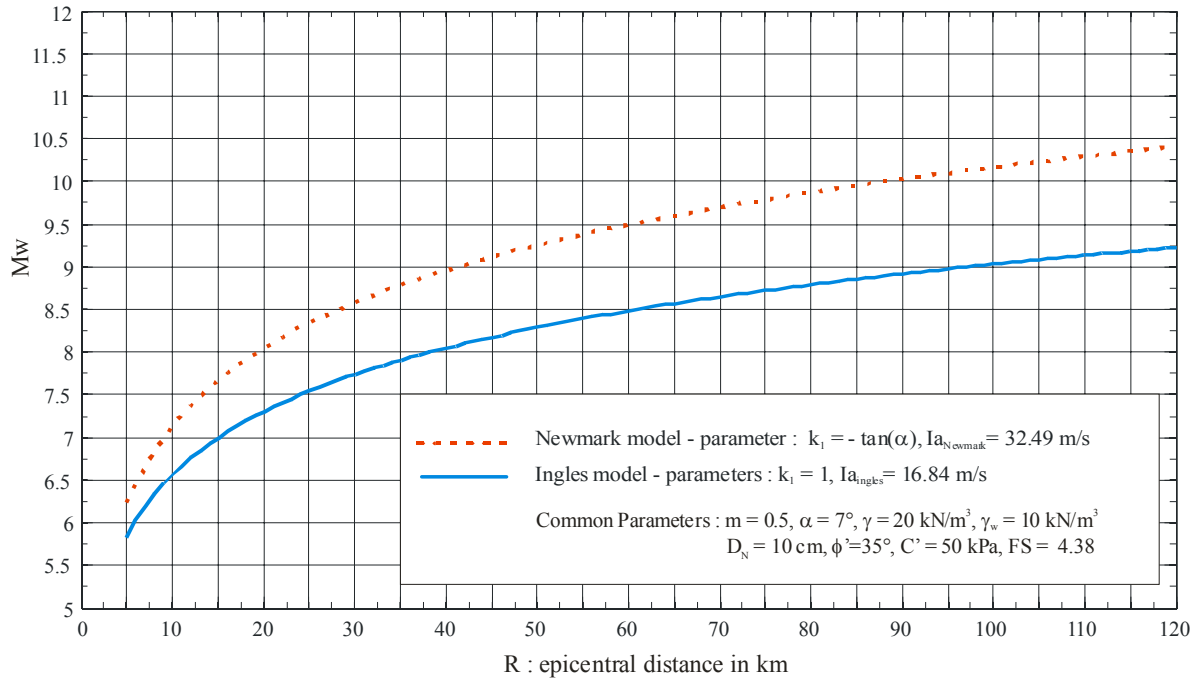


Figure 10. Variation of moment magnitude M_w versus earthquake source-distance determined from eq. (5): the critical displacement D_N is considered as 10 cm. For Ingles et al. model (2006) (solid line) we used a ratio of vertical to horizontal seismic ground acceleration $k_1 = 1$ and a resulting Arias Intensity of 16.84 m/s determined from eq. 4b. For Newmark model (1965) (dashed line) we used $k_1 = -\tan(\alpha)$ and a resulting Arias intensity of 32.49 m/s determined from eq. 4b. The common parameters used for the both models are: the ground water table $m = 0.5$, the static safety factor $FS = 4.38$ determined from eq. (2), mean slope $\alpha = 7^\circ$, the material unit weight $\gamma = 20 \text{ kN/m}^3$, the water unit weight $\gamma_w = 10 \text{ kN/m}^3$, the vertical depth of the failure surface $H = 200\text{m}$, the effective cohesion $C' = 50 \text{ kPa}$ and the effective angle of internal friction $\phi' = 35^\circ$.

The calculation of the safety factor taking into account earthquake shaking indicates that earthquakes capable of triggering the Tarapaca and other landslides of the Moquella flexure range from high magnitude shallow (or close) events ($M_w = 6.98$ at 15 km) to very high magnitude deep (far) events ($M_w = 9.2$ at 120 km). In order to check the feasibility of earthquake trigger, it is now necessary to consider the possible location of the landslide-triggering earthquakes.

The study area is presently affected by frequent high magnitude earthquakes (Delouis et al., 1996, 1997; David et al., 2002; Victor et al., 2004; Farias et al., 2005), potentially capable of triggering gently-sloping large-scale earthquakes. The recent earthquakes with magnitudes > 5 registered in the world catalogs indicate that these earthquakes are most often deep events situated along the subduction plane (Delouis et al., 1996; David et al., 2002; Victor et al., 2004; Farias et al., 2005). It would be thus envisaged as a first hypothesis that the earthquake responsible for the Tarapaca landslide and similar ones were situated on the subduction plane. If so, very high magnitude events were required. For example, if we assume a distance to the source of 50 to 120 km, the required moment magnitude will be of $M_w = 8.26$ at 50 km, M_w close to 9.0 at 100 km, and $M_w = 9.2$ at 120 km. The latter magnitudes

are greater than those of the largest events recorded since yet. The need of events with magnitude greater than the recent events is also supported by the fact that no gently-sloping large-scale landslides like these ones were associated with the largest recent events. Nevertheless, in our study area and more largely in the Andean margin between 16-22°S, several authors (Lomnitz, 1970; Kelleher, 1972; Delouis et al., 1996) recognized a seismic gap with high potential for a very high magnitude earthquake. In this case, the presence of the studied paleolandslides might be evidence that such very high magnitude event(s) may have occurred in late Cenozoic time. The localization of the megalandslides along the Moquella thrust-related “flexure” is somewhat in contradiction with very high magnitude earthquakes situated on the subduction plane, which would have produced landslides over a much larger area. As a second hypothesis, it could be envisaged that the landslides were triggered by shallow and/or nearer earthquakes generated on faults not or less active today. Shallow earthquakes with magnitudes sufficient to trigger landslides like Tarapaca might be generated by the propagation of thrust faults relating to the Moquella “flexure”. As shown by the syntectonic deposition related to the growth of the Moquella fault-related fold, tectonic activity occurred in our study area from the Miocene to the Pleistocene (Garcia, 2001; Farias et al., 2005). As pointed out earlier, the relationship between the drainage network and the landslide indicate that these landslides are aged of less than 5.5 Myr and formed during this period of tectonic activity. Today, shallow earthquakes related to the Moquella thrust are rare and magnitudes relatively low. For example, an M 6.3 earthquake with an epicentre located to the north of the Moquella thrust and a depth of 15km occurred on 04 July 2001. According to the above calculations, the magnitude of this earthquake is insufficient to form landslides comparable to Tarapaca and field studies confirm that no such landslides formed at this occasion. However, it could be reasonably envisaged that shallow earthquakes with magnitudes of $M_w 7.3$ or more occurred in the Pliocene or more recently along the Moquella thrust. The recurrence time of such large-scale events being long as shown by their scarcity in the geological record, even in the best preserved areas (see also Strasser and Schlunegger, 2005, or Philip and Ritz, 1999; Rouspignouls, 1834), the possibility of the occurrence of low-angle megalandslides as large as, or greater than, Tarapaca cannot be excluded in the future in this area or other active tectonic areas with gentle slopes *a priori* not favourable to landsliding.

CONCLUSIONS

The mega-landslides, with volumes exceeding or equal to 1 km³ are rare events only found in the geological record. The youngest ones are aged of 9500 yr (early Holocene) (see Table 1), which indicate that the recurrence time is at least ~10 kyr. Mega-landslides formed along steep (15 – 25° or more) slopes but along gentle (8 to 3°) slopes as well. The best preserved of these are low-angle soil block slides with ages between 5.5 and 2.5 Myr in the Atacama Desert (Strasser and Schlunegger; this paper) and late Pleistocene in the Gobi Desert (Philip and Ritz, 1999). This apparent paradox is easily resolved when considering that erosion has remained weak in these arid areas and is less efficient in gentle than in steep slopes.

The mega-landslides observed in the Atacama Desert are soil-block slides having large dimensions (7 km wide, 2.37 km long for the Tarapaca landslide) and gentle slopes (5° to 7-8° for the steepest Tarapaca landslide), with a thickness of the slide mass of ~200 m), which characterize them as planar landslides. The area of the transported mass is around 20-40 km² per landslide and the volume of transported sediment has been evaluated to 4.5 km³ for the Tarapaca landslide. They are bound laterally by deeply incised river valleys that form lateral free edges. The landslides are more recent than the installation of a drainage network dated of 5.5 Ma.

All the scenarios taking into account realistic variations of the static (aseismic) mechanical parameters and pore pressure values compatible with the climate of the area indicate slope stability, thus showing that earthquake shaking is necessary to the formation of the studied gently-sloping large-scale landslides.

If the safety factor is calculated by integrating earthquake shaking and the seismicity and the tectonic structure considered, it appears that earthquakes capable of triggering the Tarapaca and other landslide of the Moquella flexure might be either high-magnitude ($M_w = 6.98$) shallow events situated along the Moquella thrust zone or very high magnitude events ($M_w = 8.2$ to $M_w = 9.2$) situated along the subduction plane.

ACKNOWLEDGEMENTS

Careful critical reviews by the reviewers greatly improve the article. We are indebted to Luisa Pinto for their observations on field and Gérard Hérail for the fruitful discussions. This work was funded by Institut de Recherche et Développement, France and the University of Toulouse.

REFERENCES

- Alpers, C.N., Brimhall, G.H., "Middle Miocene climatic change in the Atacama Desert, northern Chile: Evidence from supergene mineralization at La Escondida," *Geol. Soc. Am. Bull.* 100, 1640-1656, 1988.
- Ambraseys, N.N., Simpson, K.A., "Prediction of vertical response spectra in Europe," *Earthquake Engineering and Structural Dynamics* 25, 401-412, 1996.
- Campbell, K.W., "Empirical near-source attenuation relationships for horizontal and vertical components of peak ground acceleration, peak ground velocity, and pseudo-absolute acceleration response spectra," *Seismological Research Letters*, 68, 154-179, 1997.
- Carracedo, J.C., Day, S.J., Guillou, H., Pérez Torrado, F.J., "Giant Quaternary landslides in the evolution of La Palma and El Hierro, Canary Islands," *Journal of Volcanology and Geothermal Research* 94, 169-190, 1999.
- Darroz, J., Pinto, L., Inglès, J., Soula, J.C., Maire, E., Courjault-Radé, P., Hérail, G., "Origin of the paleolandslide of Tarapaca (North Chile, Andean belt)," *Geophysical Research Abstract*, EGS02-A-03 136, 2002.
- David, C., Martinod, J., Comte, D., Hérail, G., Haessler, H., "Intracontinental seismicity and Neogene deformation of the Andean forearc in the region of Arica (18.5° S – 19.5° S)," *5th International Symposium on Andean Geodynamics*, Toulouse, Ext. Abstracts, p. 171-174, 2002.
- Delouis, B., Monfret, T., Dorbath, L., Pardo, M., Rivera, L., Comte, D., Haessler, H., Caminade, J.-P., Ponce, L., Kausel, E., Cisternas, A., "The $M_w = 8.0$ Antofagasta (northern Chile) earthquake of 30 July 1995: A precursor to the end of the large 1877 gap," *Bull. Seismol. Soc. Am.* 87, 427–445, 1997.
- Delouis, B., Cisterna, A., Dorbath, L., Rivera, L., Kausel, E., "The Andean subduction zone between 22 and 25°S (northern Chile): precise geometry and state of stress," *Tectonophysics*, 259, 81-100, 1996.
- Farias, M., Charrier, R., Comte, D., Martinod, J., Hérail, G., "Late Cenozoic deformation and uplift of the western flank of the Altiplano: Evidence from the depositional, tectonic and geomorphologic evolution and shadow seismic activity (northern Chile at 19°30'S)," *Tectonics* TC4001, doi: 10.1029/2004TC001667, 2005.
- García M., "Evolution oligo-néogène de l'Altiplano occidental (arc et avant-arc des Andes d'Arica, 18-19°S). Tectonique, volcanisme, sédimentation, géomorphologie et bilan érosion-sédimentation," PhD Thesis. Univ. Grenoble I, 286p, 2001.
- García, M.O., Sherman, S.B., Moore, G.F., Goll, R., Popova-Goll, I., Natland, J.H., Acton, G., "Frequent landslides from Koolau volcano: Results from ODP Hole 1223A," *Journal of Volcanology and Geothermal Research* 151, 251-268, 2006.

- Gregory-Wodzicki, K.M., "Uplift history of Central and Northern Andes: A review," *Geol. Soc. Am. Bull.*, 112, 1091-1105, 2000.
- Hayashi, J.N. Self, S., "A comparison of pyroclastic flow and debris avalanches mobility," *J. Geophys. Res.* 97, 9063-9071, 1992.
- Hewitt, K., "Catastrophic landslides and their effect on the Upper Indus streams, Karakoram Himalaya, northern Pakistan," *Geomorphology*, 26, 47-80, 1998.
- Hoek, E. And Bray, J., "Rock slope engineering," Institute of Mining and Metallurgy, London, 3rd edition, volume 1, 358 p., 1981.
- Ibetsberger, H.J., "The Tsergo Ri landslide: an uncommon area of high morphology activity in the Langthang valley, Nepal," *Tectonophysics*, 260, 85-93, 1996.
- Inglès, J., Darrozes, J., Soula, J.-C., "Effects of vertical component of ground shaking on earthquake-induced landslides displacements using generalized Newmark's analysis," *Engineering Geology* 86, 134-147, 2006.
- Jibson, R.W., "Predicting earthquake-induced landslide displacement using Newmark's sliding block analysis," *Transportation Research Record* 1411, 9-17, 1993.
- Jibson, R.W., "Use of landslides for paleoseismic analysis," *Engineering Geology* 43, 291-323, 1996.
- Jibson, R.W., Harp, E.L., Michael, J.A., "A method for producing digital probabilistic seismic landslide hazard map: an example from the Los Angeles, California, area," U.S. Geological Survey Open File Report, 98-113, 1998.
- Jibson, R.W., Keefer, D.K., "Analysis of the seismic origin of landslides – Examples of the New Madrid seismic zone," *Geol. Soc. Am. Bull.* 105, 421-436, 1993.
- Keefer, D.K., "Landslides caused by earthquakes," *Geol. Soc. Am. Bull.* 95, 406-421, 1984.
- Kelleher, J., "Rupture zones of south America earthquakes and some predictions," *J. Geophys. Res.* 77, 2087-2103, 1972.
- Lomnitz, C., "Major earthquakes and tsunamis in Chile during the period 1535 to 1955," *Geol. Rundsch.* 59, 938-960, 1970.
- Moon, V., Simpson, C.J., "Large-scale mass wasting in ancient volcanic material," *Engineering Geology* 64, 41-64, 2002.
- Moore, J.G., Clague, D.A., Holcomb, R.T., Lipman, P.W., Normark, W.R., Torresan, M.E., "Prodigious submarine landslides on the Hawaiian ridge," *J. Geophys. Res.* 94, 17,465-17, 484, 1989.
- Moore, J.G., Normark, W.R., Holcomb, R.T., "Giant Hawaiian landslides," *Ann. Rev. Earth Planet. Sci.*, 22, 119-144, 1994.
- Muñoz, N., Sepúlveda, P., "Nota Geologica : Estructuras compresiva con vergencia al oeste en el borde oriental de la Depression Central, Norte de Chile (19° 15' S)," *Revista Geológica de Chile* 19, 91-103, 1992.
- Naranjo, J.A., Paskoff, I., "Evolution Cenozoica del piemonte andino en la Pampa del Tamagural, norte de Chile (18°-21° S)." IV Congreso Geologico Chileno, 4, 149-165, 1985.
- Newmark, N.M., "Effects of earthquakes on dams and embankments," *Geotechnique* 15, 139-159, 1965.
- Newmark, N.M., Hall, W.J., "Earthquake Spectra and Design," Earthquake Engineering Research Institute, Berkeley, 1982.
- Philip, H., Ritz, J.F., "Gigantic paleolandslide associated with active faulting along the Bogd fault (Gobi-Altay, Mongolia)," *Geology* 27, 211-214, 1999.
- Pollet, N., "Mouvements gravitaires rapides des grandes masses rocheuses : apport des observations de terrain à la compréhension des processus de propagation et de dépôt. Application aux cas de la Madeleine (Savoie, France), Flims (Grisons, Suisse) et Köfels

- (Tyrol, Autriche),” PhD thesis, Ecole nationale des Ponts et Chaussées, Paris.
<http://pastel.paristech.org/bib/archive/00000820/>, 2004.
- Rouspignouls, S., “Vision sur les grands glissements”, Soc. Hist. Nat. De Toul., 32-35, 1834.
- Schramm, J.M., Weidinger, J.T., Ibetsberger, H.J., “Petrologic and structural control on geomorphology of prehistoric Tsergo Ri slope failure, Lanthang Himal, Nepal,” *Geomorphology* 26, 107-121, 1998.
- Skempton, A.V., Hutchinson, J.N., “Stability of natural slopes and embankment foundations. State of art report,” 7th Conf. Soil Mech. Found. Eng., Mexico, 291-335, 1969.
- Stasser, M., Schlunegger, F., “Erosional processes, topographic length-scale and geomorphic evolution in arid climatic environments: the ‘Lluta collapse’, northern Chile. *Int. J. Earth Sci. (Geol. Rundsch.)* 94, 433-446, 2005.
- Stillmann, C.J., “Giant Miocene landslides and the evolution of Fuerteventura, Canary Islands,” *Journal of Volcanology and Geothermal Research*, 94, 89-104, 1999
- Summerfield, M.A., “Global Geomorphology, an introduction to the study of landforms,” Longman Sci. and Tech, U.K./John Wiley & Sons, New York, N.Y., 357p., 1991.
- Vargas, G., Ortlieb, L., Rutilant, J., “Aluviones historicos en Antofagasta y su relacion con eventos El Niño/Oscilacion del Sur -,” *Revista. Geológica de Chile* 27, 157-176, 2000.
- Victor, P., Oncken, O., Glodny, J., “Uplift of the Altiplano plateau: evidence from the Precordillera between 20 and 21°S (northern Chile),” *Tectonics* 23, TC 4004 doi:10.1029/2003TC001519, 2004.
- Voight, B. (Ed), “Rockslides and Avalanches. I. Natural phenomena,” Elsevier, New York, 1978.
- Wieczorek, G.F., Wilson, R.C., Harp, E.L., “Map showing slope sability during earthquakes of San Mateo County, California,” U.S. Geological Survey Miscellaneous Geologic Investigation Map I-1257E, scale 1.62,500, 1985.
- Wilson, R.C., Keefer, D.K., “Predicting areal limits of earthquake-induced landsliding, in: J.I. Ziony (Ed), *Evaluating Earthquake Hazards in the Los Angeles Region – An Earth-Science Perspective*,” U.S. Geological Survey Professional Paper 1360, 316-345, 1985.